

# Ten Overdensities and an Arc Structure in the Galactic Halo

C. Liu<sup>1,2\*</sup>, J. Hu<sup>1</sup>, and Y. Zhao<sup>1</sup>

<sup>1</sup> National Astronomical Observatories, Chinese Academy of Sciences, Beijing 100012, China

<sup>2</sup> Graduate University of Chinese Academy of Sciences, Beijing 100049, China

Received ; accepted

## ABSTRACT

**Aims.** We use Sloan Digital Sky Survey (SDSS) DR5 photometric data to explore the structure of the Galaxy halo and hope to discover new companions or substructures which may reveal the forming history of the halo.

**Methods.** We study overdensities in a sky area where  $\alpha = 120^\circ \sim 270^\circ$  and  $\delta = 25^\circ \sim 70^\circ$  and pick out ten overdensity areas by comparing color-magnitude diagrams with known globular clusters or dwarf spheroidal galaxies. An automatic template matching method is developed to fit the color-magnitude diagram for each overdensities with a suitable stellar evolution isochronic line so that distance module and metalicity are roughly estimated. The performance test of the method indicates that our estimates on distance is acceptable.

**Results.** The 10 overdensities and three known objects, UMa I, UMa II and Willman 1 are found to be connected with a long arc substructure starts from  $\sim 8$ kpc above the disk and spread to  $\sim 150$ kpc into north galactic cap. Evidence also shows a relationship between metalicities and distance modules of the overdensities.

**Conclusions.** C7, one of the 10 overdensities is most likely a dwarf spheroidal galaxy according to radial density profile study and its absolute magnitude. Other overdensties are not classified for poor information. The arc structure may either be a long tidal stream or be an intrinsic substructure of the halo. Follow-up study need to be done to clarify this problem.

**Key words.** Galaxy: structure – Galaxy: halo – galaxies: dwarf – Local Group

## 1. Introduction

Tidal streams in the Milky Way attributed to accretion of smaller galaxies nearby support the hierarchical merging cosmogonies(Lynden-Bell & Lynden-Bell 1995). After discovered the large-scale tidal arms due to Sagittarius dwarf spheroidal galaxy accretion events (Yanny et al. 2003; Majewski et al. 2003 and Rocha-Pinto et al. 2004), more tidal streams are detected from Sloan Digital Sky Survey (SDSS; York et al. 2000) data. Remarkably strong tidal tails of Palomar 5 are discovered by Odenkirchen et al. 2001, Rockosi et al. 2002 and Grillmair & Dionatos 2006. Another tidal tails are connected with NGC5466 (Belokurov et al. 2006a; Grillmair & Johnson 2006). Belokurov et al. 2006b reveals an area of so-called *Field of Streams*, which contains not only Sagittarius arms but also Virgo overdensity (Jurić et al. 2005), Monoceros Ring (Newberg et al. 2002), Orphan stream and a  $60^\circ$ -long stream between Ursa Major and Sextans (Grillmair 2006b; we call it GD-1 in this paper). The fact that tidal streams are often associated with globular clusters or dwarf spheroidal galaxies implies that it is possible to search for tidal streams by identifying new faint satellite dwarf galaxies and globular clusters or remnants of them.

New satellite companions of the Milky Way have been discovered in the recent years. About 150 globular clusters (Harris 1996) and 9 widely-accepted dwarf spheroidal galaxies (dSph) (Belokurov et al. 2006d) are known before SDSS. Big progress are made after using SDSS data since 2005. At least nine new companions are discovered within two years. Seven of them are dSph satellites: Ursa Major I (Willman et al. 2005a), Canes Venatici

I(Zucker et al. 2006a), Boötes (Belokurov et al. 2006c), Ursa Major II (Zucker et al. 2006b; Grillmair 2006a), Coma Berenics, Canes Venatici II, Hercules and Leo IV (Belokurov et al. 2006d). Two of them are probably globular clusters: Willman 1 (Willman et al. 2005b) and Seque 1 (Belokurov et al. 2006d).

It is impossible to recognize these objects from SDSS images since they are resolved into field stars. Fortunately, they can be found by detecting locally overdensities in SDSS stellar databases (Belokurov et al. 2006d) by adding some constraints on magnitude and color index. Overdensity study is a prompt data mining method to find more unknown satellite galaxies or globular clusters. We use a similar method with Belokurov et al. 2006c but utilize different parameters to scan a sky area of  $\alpha = 120^\circ \sim 270^\circ$ ,  $\delta = 25^\circ \sim 70^\circ$  and observe ten interesting overdensities, which color-magnitude diagrams similar with a globular cluster or a dSph. They are candidates of globular clusters or dSphs or at least clumps on the tidal streams due to dSphs. After estimating their heliocentric distance, a 3D space plotting is available and a dramatically long arc composed by these overdensities and 3 known satellites objects are revealed. Follow up observations should be helpful on ensuring if it is a tidal stream or other unknown structure in the galactic halo.

The organization of this paper is as follows. The section 2 describes the method of searching for candidates. Data acquisition and reduction process and candidates discovery are mentioned in the first subsection. A template matching algorithm for estimating properties of the overdensities is described in the next subsection. Then we discuss the performance of distance estimation of the algorithm in subsection 4. A rough measurement of radial density profile are addressed in subsection 5. In section 3 we illustrate what the overdensities possibly are. Then we show

\* email: chaoliu@lamost.org

the arc structure connected with them and 3 known satellites. A short conclusion of this paper are arranged at the last session.

## 2. Discovery

### 2.1. Data Acquisition and Reduction

SDSS DR5 provides  $u$ ,  $g$ ,  $r$ ,  $i$ ,  $z$  bands (Fukugita et al. 1996) photometric data and covers 8000 degs<sup>2</sup> (Adelman-McCarthy et al. 2006). It classifies the objects into several classes. Stellar objects are used in our task. We select a data set from SDSS databases. SDSS considers all point sources as stars, including quasars and faint galaxies. This is one of the contaminant sources when we are identifying the Milky Way companions by color magnitude diagrams. An alternative contaminant is bright galaxies. In order to decrease the affects of the contaminants during data analysis  $i$  band magnitude are limited between 19 and 22 and color  $g - i$  are limited between 0 and 1. The location limitation are also necessary for the data set to avoid Sagittarius dwarf spheroidal galaxy's tidal arms. A range of  $\alpha = 120^\circ \sim 270^\circ$  and  $\delta = 25^\circ \sim 70^\circ$  are used to query all star type data from SDSS Casjobs<sup>1</sup> and approximately  $3.6 \times 10^7$  objects are obtained. In each band, extinctions are subtracted using values provided by SDSS database, which are computed following Schlegel et al. 1998.

The sky area we detect is binned by  $0.05^\circ \times 0.05^\circ$  to compute star count density. Hence,  $750 \times 225$  bins are generated. Only those whose density is  $2\sigma$  higher than its field mean density are interesting. Field mean density and standard deviation for each bin are defined by the corresponding value of a  $11 \times 11$  window surrounded.

525 overdensity bins are obtained during this process. All known globular clusters and dSphs located in the detecting sky area, UMa II, UMa I, Willman 1, Pal4, CVn II, CVn I, NGC5272, NGC5466, NGC6205, NGC6341, Draco, and Leo III, are included, some of which cover more than 2 bins for their bigger scale. Contaminants comes from bright galaxies, cluster of galaxies, and bright stars are recognized and eliminated from the collection. The overdensity bins close to the detection boundaries (less than  $0.5^\circ$ ) are also ignored. The rest overdensities are studied with their density diagrams and color-magnitude diagrams (CMD).

Density contour diagram and CMD are generated by stars within a  $1^\circ \times 1^\circ$  area centered at each overdensity bins. 9 known objects, including Pal 4, UMa I, UMa II, CVn I, Draco, NGC 6341, NGC 5466, Willman 1 and NGC 6205, are selected to be templates for identifications. The distance module (DM) distribution of these templates covers from 14.2mag to 21.7mag. This ensures that the templates covers all CMD's morphological features. Ten most similar overdensities are finally picked out from almost 500 samples by comparing with templates. Figure 1-Figure 2 display density contours, center area (circle with  $r = 0.1^\circ$  or  $r = 0.15^\circ$ ) CMDs, field (annuli area between  $r = 0.5^\circ$  and  $r = 0.6^\circ$ ) CMDs and Hess contours (subtraction between corresponding center area CMDs and field CMDs with normalized star counts).

### 2.2. Template Matching Method for Parameter Estimate

An automatic template matching algorithm is used to find out the best fitted Padova isochrone lines (Girardi et al. 2004) for each candidate. Stellar evolution isochrone lines are converted

to masks where the color  $g - i$  changes from -1 to 2 with step of 0.03 and the magnitude  $i$  changes from -10 to 10 with step of 0.1. Thus a binary  $100 \times 200$  image mask for each isochrone line is formed. The value of each item in the image is either 1 (represents for neighbour area of isochrone line) or 0 (represents for area far away from isochrone line). Changing metalicity, age and distance module values, a series of mask templates are formed. For each candidate's Hess diagram, compute value  $R$  using following formula:

$$R = \frac{\sum_{g-i,i} (C(g-i,i)(1 - T(g-i,i, Z, A, DM)))}{\sum_{g-i,i} C(g-i,i)} \quad (1)$$

where  $C(g - i, i)$  is the candidate's Hess diagram ( $i = 13 - 22$ mag).  $T(g - i, i, Z, A, DM)$  is a template mask with specific metalicity  $Z$ , age  $A$  and distance module  $DM$ . The value of  $Z$  has options of 0.0001, 0.0004, 0.001, and 0.004. The value of  $A$ , in  $\log_{10}(yr)$ , changes from 9.5 to 10.25 with a step of 0.05. And the value of  $DM$  changes from 13mag to 21.9mag with a step of 0.1mag. Totally there are 5760 templates tried on each overdensities. It is obviously that the smaller the  $R$  has the higher the template matches the overdensity. The template minimizes  $R$  are selected as the matched one.

### 2.3. Distances of the Overdensities

Matched isochrone lines are overlapped onto the Hess diagrams of overdensities in Figure 1-2. Distance modules of the matched templates are considered as roughly estimation of the overdensities. For isochrone line fitting cannot determine precise age and metalicity (see following discussion), we just treat ages and metalicity from the method as order estimation of the overdensities. Table 1 displays the parameters of the matching templates for each overdensities.

We use 9 known globular clusters and dwarf spheroidal galaxies, UMa I & II, CVn I & II, Pal4, NGC6205, NGC5466, NGC5272, and NGC6341, as samples to test the performance of the algorithm. They are all located in the detected area and all be detected during our overdensity selecting process. Their distance modules cover from 14 to 22, which have been estimated by others who used different methods (which are listed in Table 2). The performance can be measured by

$$\sigma = \sqrt{\sum \frac{(DM_t(i) - DM_0(i))^2}{N}} \quad (2)$$

where  $DM_t(i)$  is the distance module of the  $i$ th test sample computed from template matching method;  $DM_0(i)$  is the distance module of the  $i$ th testing sample come from related references;  $N$  is the count of testing samples. Table 2 shows both distance determination results for testing samples. We get  $\sigma = 0.23$ . The isochrones we use in our algorithm would not provide a precise estimation on distance because they are conducted with an assumption of single stellar population. Hence, our  $\sigma$  value is acceptable.

Measurement to the clear features of overdensities' CMD shows another independent way to estimate the distance. The distances of C3, C4, C5, C7, C8, C9 and C10 are approximately estimated by their possible HB feature. We assume that horizontal branch has a same luminosity with RR Lyrae. That is,  $M_V = 0.7$ mag and  $B - V = 0.38$ mag for all HB star (Cox 2000). The transformation from  $V$  and  $B - V$  to SDSS photometric system follows Fukugita et al. 1996 is:

$$g = V + 0.56(B - V) - 0.12 \quad (3)$$

<sup>1</sup> <http://casjobs.sdss.org/dr5/en/>

The absolute magnitude in band  $i$  of HBs can be estimated by subtraction of  $g$  got from the formula 3 and the color  $g - i$ . All these estimate results are displayed in Table 2. The matched template's distance parameters are also listed in the Table 2 for comparison.

#### 2.4. Density profiles

Stars which are filtered by overdensities' Hess contours showed in the right most column in Figure 1-2 are used to generate density profiles(Figure 3-6). We use nonparametric density estimation to fit a density distribution function of each overdensities. The isodensity contours are displayed in Figure 3-6. We use density-weighted first moments to derive centroids (Belokurov et al. 2006c) (listed at the first two columns of Table 1). We rotate a line across the centroids of each overdensity and compute the integral of the densities along with the line at every angles. We treat the angle that maximizes the sum as the position angle. We consequently fit the major axis radial profile with King model (King 1962). Considering  $R^2 \geq 0.85$  as the criteria of the goodness of the fitting, C1, C2, C3, C7 and C10 are fitted well whereas C4, C5, C6, C8 and C9 are not. Parameters are listed in table 4 and density profile diagrams are displayed in Figure 7-10.

### 3. Discussion

#### 3.1. What Are The Overdensities?

The concentration ratio  $c = \log(r_t/r_c)$  (King 1962) and line scale are important features to distinguish what the overdensities are. C7 has the highest  $c=0.47$  among 10 overdensities and a line scale of  $\sim 593$ pc in half light radius ( $r_c$  in Table 4). As comparison, Draco has  $c = 0.5$ , Leo II has  $c = 0.48$  and Fornax has a similar size of  $r_{c,g} = 400$ pc(Irwan & Hatzidimitriou 1995). The absolute magnitude of C7 is computed by adding all luminosity values of stars within  $r_c$  twice and then subtracting distance module. Following Fukugita et al. 1996, we transform  $r$  band to  $V$  band and get  $M_V \sim -8.04$ mag. Thus, the location of C7 on  $r_h - M_V$  plane is very close to CVn I (Belokurov et al. 2006d). These evidences reveal that C7 is most likely a dwarf spheroidal galaxy.

Other overdensities has very low  $c$  which indicates that they are probably disrupted or too faint to be observed sufficient stars. The line scales of C1 and C2 are comparable with globular clusters ( $r_h < 25$ pc; Harris 1996). Considering their lower concentration ratio than normal globular clusters ( $c > 0.5$ ; Harris 1996), they are most likely disrupted globular clusters.

C3 and C10 are fitted by King model. However, their concentration ratio are far lower than either dSphs or globular clusters. Their line scales are comparable with dSphs. They are most likely clumps on some tidal streams due to dwarf galaxies.

C4, C5, C6, C8 and C9 do not be fitted by King model. There several possible reasons listed below. First, some overdensities' angle scales are so small and the data we used cannot provide enough resolution to measure their radial profiles. Second, field star contaminants are significant to these overdensities so that we cannot subtract them completely. Field stars let the outer radius profile too blur to estimate the tidal radius  $r_t$  of King model. Third, these overdensities themselves are not gravity systems. They should be clumps on some tidal stream due to dwarf galaxies. We prefer to the first reason for C4, C6 and C9 because these three overdensities display a compact core on their isodensity profiles in Figure 4 and 5 and their radial profile is clear but with

only a few values which cannot get a precise fitting result. We prefer to the second reason for C5 because its isodensity profile is scattered than other overdensities and its radial profile shows more distributions. We prefer to the last reason for C8 for its isodensity profile show unusual two cores which is obviously different from either globular cluster or dwarf spheroidal galaxy. It is likely a remnant of a dSph.

#### 3.2. The Arc Structure

We plot the overdensities and all known dSphs and globular clusters located in the detected area in a same 3D space as showed in Figure 11. A dramatic arc structure, which is composed by 9 of our overdensities and 3 known satellites, UMa I, UMa II and Willman 1, is revealed. The nearest end of the arc is at C1 and C2, which are both 13.8kpc away from the Sun and 7.6kpc(C1), 7.8kpc(C2) high above the galactic disk. The farthest end of the arc is at C8, which is 166kpc away from the Sun and 147kpc high above the disk. Overdensities C1-C9 and UMa I & II and Willman 1 are proximately arranged along a straight line on YZ plane. Hence, we suppose that the arc is located on a plane which perpendicular to YZ plane and use a 2-order polynomial to fit the 12 objects. The fitted curve are overlapped to 3D plotting and projected plotting in Figure 11. The related coefficient reaches more than 90% which implies the fitted curve is highly related to the 12 satellites.

Willman et al. 2005a estimated that UMa I has  $M_V = -7.0$ , while C7 has  $M_V \sim -8.04$ . Thus UMa I and C7 may be two of the biggest objects among the 12 arc composers. Is one of them the progenitor of the big arc? We cannot answer this question depending on the current results. Follow-up observations should be done to confirm: 1) if the overdensities and the satellites on the arc are related to each other in the aspect of stellar population or in the aspect of kinematics; 2) if or not the UMa I or C7 is the progenitor after 1) is confirmed.

We plot all known tidal stream in our detected area in a same galactic coordinates and overlap the arc and its composers(see Figure 12) in order to search if there is any connection between the arc and known tidal streams.

C1, C2, C6 and UMa II are overlapped by Monoceros Ring. However, following Newberg et al. 2002, the Monoceros Ring is located at 8kpc away from the Sun, nearer than C1, C2 and C6. Consequently, we eliminate the suppose that C1, C2 and C6 belong to Monoceros Ring.

Orphan stream are close to the arc and seems have a same direction with it. Based on Fellhauer et al. 2006, the Orphan stream is almost perpendicular to the sight of light and located at  $\sim 30$ kpc away from the sun near UMa II. And their simulation results support that UMa II is related to Orphan stream. The relationship between Orphan stream and the arc is another open problem needs to be solve rely on follow-up observations.

#### 3.3. Age and Metalicity

The template matching method for Hess diagram does not produce precise age estimate for two reasons. First the turnoff and SGB, which are sensitive to age, are not as abundance as main sequence stars. Thus, they are weak and easily be resolved by field stars. Second, most our overdensities are either far away so that not clear TO features appear in Hess contours or too faint to show the features because of disruption.

We use four known dwarf galaxies, UMa I, UMa II, CVn I and CVn II, to test if the template match-

ing method can be used to estimate metalicity. Figure 13 (a) shows the comparison of our algorithm and values from literatures (Zucker et al. 2006b, Willman et al. 2005a, Belokurov et al. 2006d and Zucker et al. 2006a) It indicates that our method can be used to estimate the order of the metalicity but not for precise value.

We then study the relationship between metalicity and distance module of the ten overdensities and get a trend showing in figure 13 (b). It shows that the metalicities are decreasing when the distance of dSphs and our overdensities are increasing. However, not all 5 globular cluster occurs in the same sky area, NGC5272, NGC5466, NGC6205, NGC6341 and Pal4, comply with this relationship (Harris 1996 and Stetson et al. 1999).

There are two possible explanations about this relationship. First, if the arc structure has a velocity toward the galactic disk, this relationship may implies that a metalicity graduate exists into the progenitor. The outer side of the dwarf galaxy has poor metal while the inner side contains richer metal. Luminosity segregation assumption requires the head of the stream, C1, C2 and C6, should contains more giant stars. However, we do not find the abundance of RGBs or AGBs in C1 and C2's CMD is higher than other overdensities.

Another possible explanation is that if the arc structure is running away from the disk, that means at some time in the past, the progenitor crossed through the Milky Way's disk and move away from us. The near end of the arc may be polluted by dust spread on the disk when collapse occurs. It consequently shows richer metalicity than the same stellar population counterparts. The progenitor should be found at the far end of the arc in this case. If UMa I or C7 is the progenitor it will support this hypothesis. Besides, the tidal tail of the stream, since they come from the shell of the progenitor, may be lack of giant stars because of luminosity segregation. The lack of AGBs and RGBs in C1, C2 and C6 also supports this hypothesis.

Follow-up study, either observations or numerical simulations should be done so that the answer of this problem can be revealed.

## 4. Conclusions

In this paper we report ten interesting overdensities detected from SDSS database. They show features similar with globular clusters or dSphs in their CMDs. The density profiles and absolute magnitude indicates that C7 is likely a dSph, while other overdensities' type are not cleared because the limitation of SDSS data. 3D space plotting reveals a remarkable arc structure composed by 9 of the overdensities and three known galaxy satellites, UMa I, UMa II and Willman 1.

The arc structure is likely a tidal stream. If it is the case, UMa I or C7 is probably the progenitor. This needs to be proved by future works.

We also find that the 10 overdensities and 4 known dSphs located in our detected sky area comply with a linear relationship of metalicity versus distance, while globular clusters do not comply with it. We give two possible explanations of this relationship and also need some future work to prove them.

## References

Adelman-McCarthy, J., et al., 2006, ApJS, submitted  
 Cox, A. N. ed., 2000, Allen's Astrophysical Quantities (4th edition), Springer-Verlag New York Inc., p.400  
 Belokurov L., et al., 2006a, ApJ, 637, L29  
 Belokurov L., et al., 2006b, ApJ, 642, L137  
 Belokurov L., et al., 2006c, ApJ, 647, L111  
 Belokurov L., et al., 2006d, ApJ, submitted astro-ph/0608448  
 Bergbusch, P. S., & VandenBerg, D. A., 1992, ApJS, 81, 163  
 Fukugita, M., et al., 1996, AJ, 111, 1748  
 Fellhauer, M., et al., 2006, MNRAS, submitted astro-ph/0611157  
 Grillmair, C. J., & Dionatos, O. 2006, ApJ, 641, L37  
 Grillmair, C. J., & Johnson, R. 2006, ApJ, 639, L17  
 Grillmair, C. J., 2006a ApJ, 645, L37  
 Grillmair, C. J., 2006b ApJ, 651, L29  
 Girardi L., et al., 2004 A&A, 422, 205  
 Harris, W. E., 1996, AJ, 112, 1487  
 Irwin, M., & Hatzidimitriou, D., 1995, MNRAS, 277, 1354  
 Jurić, M., et al., 2005 ApJ, submitted astro-ph/0510520  
 King, I., 1962, AJ, 67, 471  
 Lee, Y.-W., Demarque, P., Zinn, R., 1990, ApJ, 350, 155  
 Lynden-Bell, D., & Lynden-Bell, R. M., 1995, MNRAS, 275, 429  
 Majewski, S. R., et al., 2003, ApJ, 599, 1082  
 Newberg, H. J., et al. 2002, ApJ, 569, 245  
 Odenkirchen, M., et al. 2001, ApJ, 548, L165  
 Rocha-Pinto, et al., 2004, ApJ, 615, 732  
 Rockosi, C. M., et al. 2002, AJ, 124, 349  
 Schlegel, D. J., Finkbeiner, D. P., & Davix, M., 1998 ApJ, 500, 525  
 Stetson, P. B., et al., 1999, AJ, 117, 247  
 Willman, B., et al., ApJ, 626, L85  
 Willman, B., et al., AJ, 129, 2692  
 Yanny, B., et al., 2003, ApJ, 588, 824  
 York, D. G., et al., 2000 AJ, 120, 1579  
 Zucker, D. B., et al., 2004 ApJ, 612, L121  
 Zucker, D. B., et al., 2006a ApJ, 643, L103  
 Zucker, D. B., et al., 2006b ApJ, 650, L41

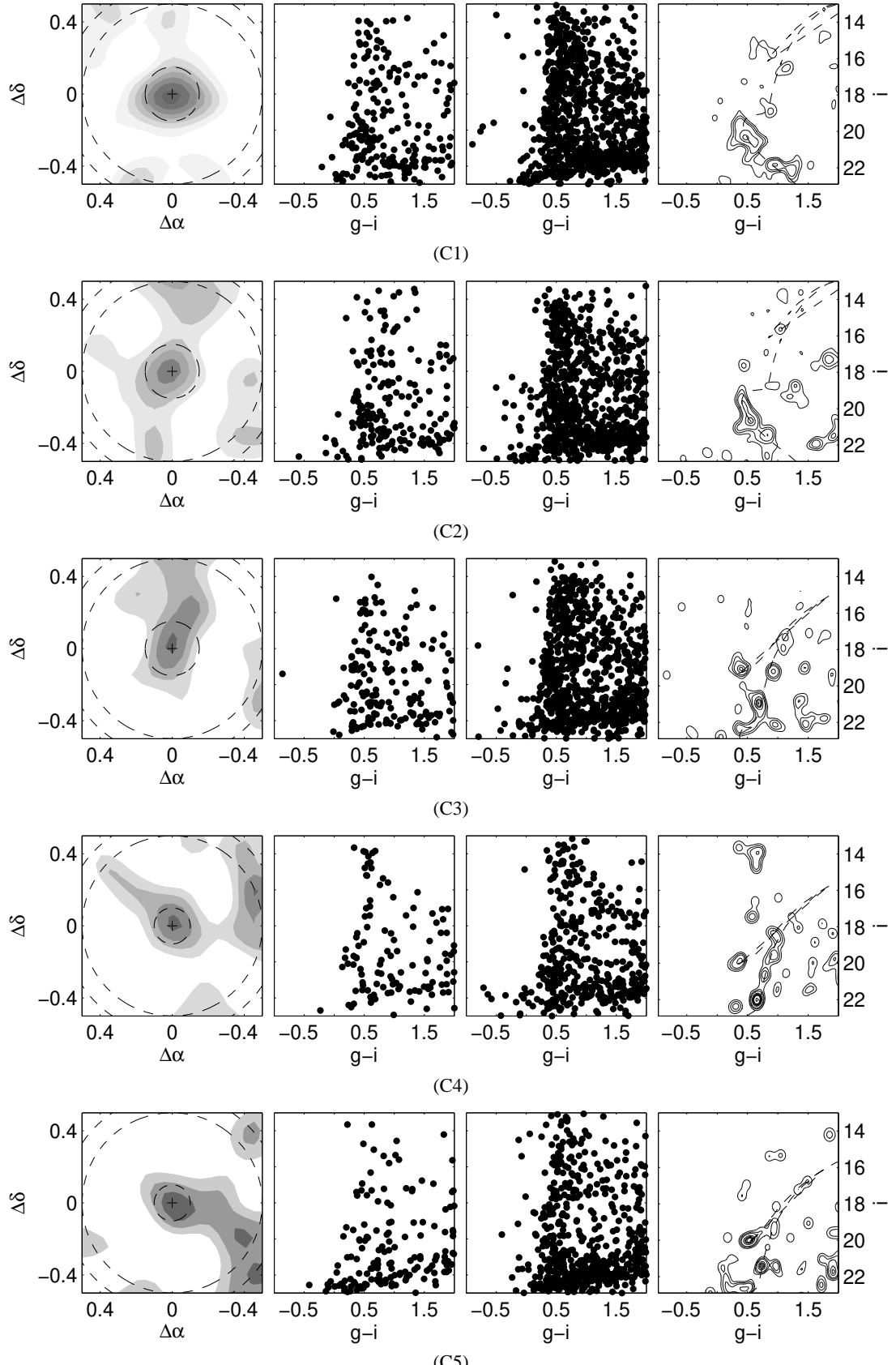


**Fig. 1.** The first five overdensities labeled from C1 to C5. The first column of diagrams are density images. The samples located in the  $1^\circ \times 1^\circ$  area around overdensities are clipped by a magnitude range  $i = 19 \sim 22$ mag and color range  $g - i = 0 \sim 1$ mag. Each density contour are constructed by nonparametric distribution density estimates with a Gaussian kernel and a window of  $0.1^\circ$ . The second column of diagrams display overdensities CMDs. Points in this column are samples from the smallest circle ( $r = 0.1^\circ$  or  $0.15^\circ$ ) overlapped on density contours. The third column of diagrams display field CMDs for each overdensities. Points in this column are samples from the intermediate circle ( $r = 0.5^\circ$ ) and the biggest circle ( $r = 0.6^\circ$ ). The right most column of diagrams are Hess diagrams which are results of subtraction between the overdensities CMDs and corresponding field CMDs. Contour levels are 1, 2, 3, 5, 6, 6.5, and  $7\sigma$  above the background. Best fitted stellar evolution isochrones are overlapped in Hess diagrams with

**Table 1.** Parameters of matched stellar evolution isochrone for each overdensities.

| No. | RA<br>(J2000) | DEC<br>(J2000) | Z      | Age<br>( $\log_{10}(yr)$ ) | m-M<br>(mag) |
|-----|---------------|----------------|--------|----------------------------|--------------|
| C1  | 123.432°      | +51.091°       | 0.004  | 10.05                      | 15.7         |
| C2  | 125.366°      | +56.148°       | 0.004  | 10                         | 15.7         |
| C3  | 127.233°      | +57.164°       | 0.001  | 10.2                       | 18.7         |
| C4  | 145.004°      | +66.631°       | 0.001  | 10.2                       | 19.4         |
| C5  | 150.044°      | +57.580°       | 0.001  | 10.15                      | 19.6         |
| C6  | 164.505°      | +28.734°       | 0.004  | 9.95                       | 16.9         |
| C7  | 174.210°      | +58.782°       | 0.0004 | 10.15                      | 20.4         |
| C8  | 193.444°      | +55.056°       | 0.0004 | 10.05                      | 21.1         |
| C9  | 194.170°      | +63.485°       | 0.0001 | 10.05                      | 20.8         |
| C10 | 202.217°      | +28.631°       | 0.0004 | 10.1                       | 19.4         |

**Table 2.** Comparison of distances from template matching method and from other's works

| Name    | DM from template<br>(mag) | DM from references<br>(mag0) | references            |
|---------|---------------------------|------------------------------|-----------------------|
| UMa II  | 17.9                      | 17.5                         | Zucker et al. 2006b   |
| UMa I   | 19.9                      | 20                           | Willman et al. 2005a  |
| Pal4    | 20.2                      | 20.02                        | Harris 1996           |
| CVn II  | 20.9                      | 20.9                         | Blokurov et al. 2006d |
| CVn I   | 21.7                      | 21.75                        | Zucker et al. 2006a   |
| NGC5272 | 15                        | 15.04                        | Harris 1996           |
| NGC5466 | 16.1                      | 16.1                         | Harris 1996           |
| NGC6205 | 14.7                      | 14.28                        | Harris 1996           |
| NGC6341 | 14.9                      | 14.59                        | Harris 1996           |

**Table 3.** Position information of overdensities.

| No. | I<br>(deg) | b<br>(deg) | Distance 1*<br>(kpc) | Distance 2**<br>(kpc)   |
|-----|------------|------------|----------------------|-------------------------|
| C1  | 167.743    | 33.454     | -                    | $13.8^{+1.5}_{-1.4}$    |
| C2  | 161.651    | 34.644     | -                    | $13.8^{+1.5}_{-1.4}$    |
| C3  | 160.342    | 35.613     | 54.6                 | $55.0^{+6.1}_{-5.5}$    |
| C4  | 145.848    | 40.955     | 77.9                 | $75.9^{+8.5}_{-7.6}$    |
| C5  | 155.432    | 47.302     | 88.6                 | $83.2^{+9.3}_{-8.4}$    |
| C6  | 202.592    | 64.956     | -                    | $24.0^{+2.7}_{-2.4}$    |
| C7  | 140.078    | 55.795     | 116.8                | $120.2^{+13.4}_{-12.1}$ |
| C8  | 122.216    | 62.071     | 159.0                | $166.0^{+18.1}_{-16.7}$ |
| C9  | 121.944    | 53.636     | 141.1                | $144.5^{+16.2}_{-14.5}$ |
| C10 | 45.384     | 81.597     | 82.7                 | $75.9^{+8.6}_{-7.6}$    |

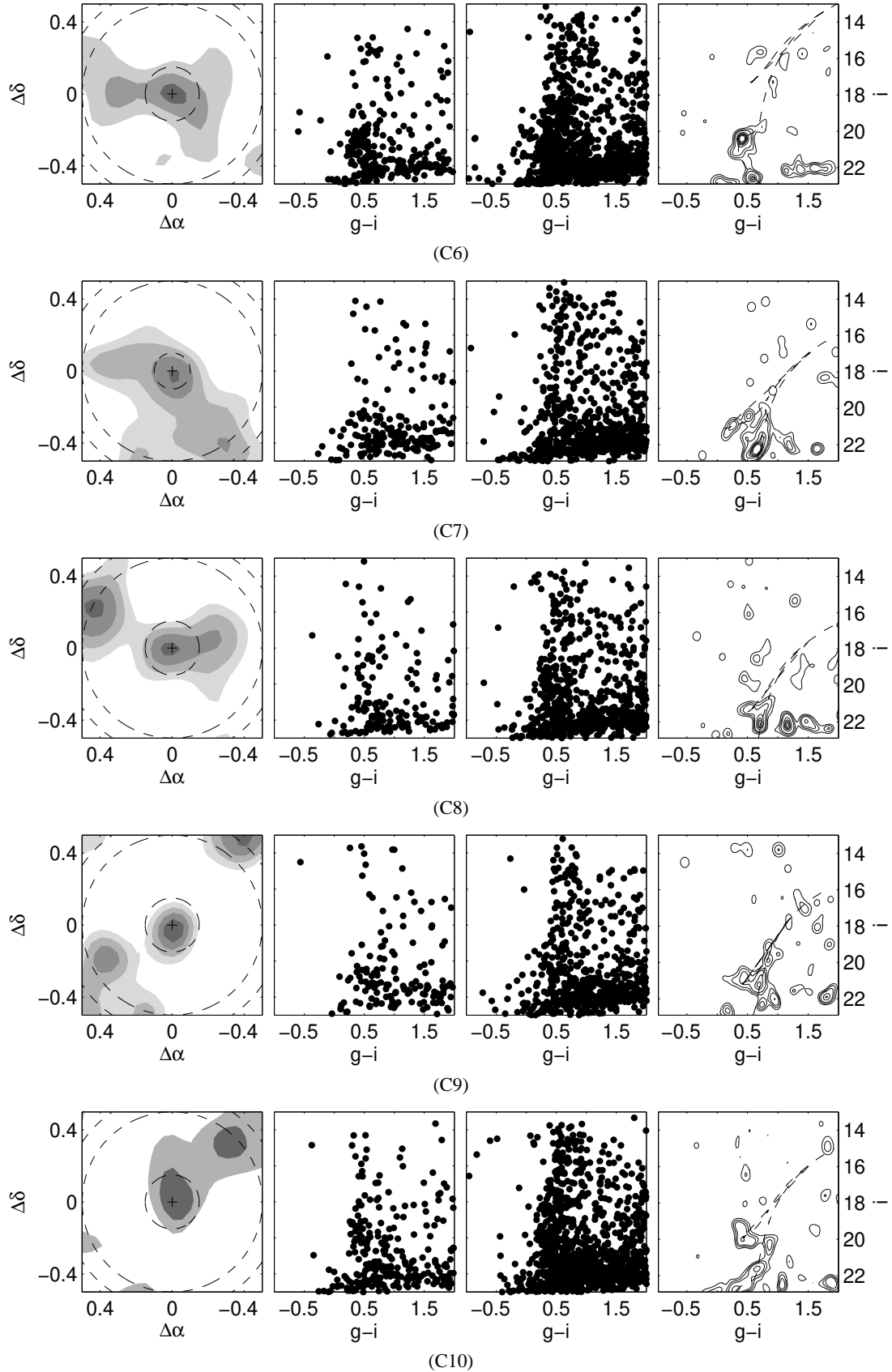
\* estimated by HB

\*\* estimated by template

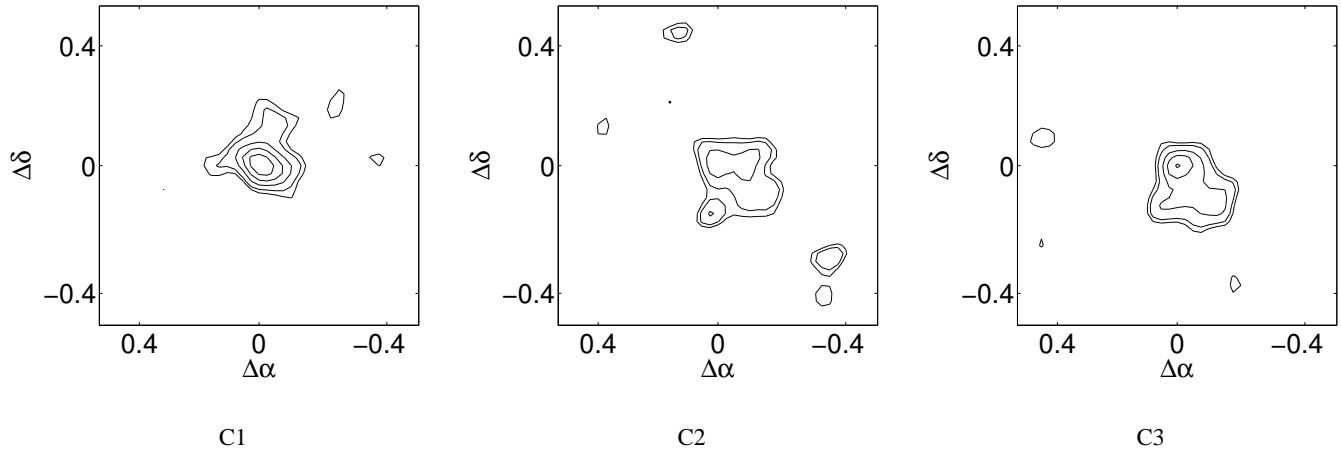
**Table 4.** Density radial profile parameters

| No. | e   | pa<br>(deg)      | $r_c$<br>(arcmin) | $r_t$<br>(arcmin) | $R^2$ | c               | $r_{c,g}$<br>(pc) |
|-----|-----|------------------|-------------------|-------------------|-------|-----------------|-------------------|
|     |     |                  |                   |                   |       | $\log(r_t/r_c)$ |                   |
| C1  | 0.3 | $37.5 \pm 10.5$  | $11.16 \pm 2.61$  | $20.34 \pm 3.01$  | 0.911 | 0.26            | $\sim 44.8$       |
| C2  | 0.1 | $45.5 \pm 2.5$   | $19.51 \pm 8.93$  | $35.31 \pm 14.15$ | 0.877 | 0.26            | $\sim 78.3$       |
| C3  | 0.1 | $-24.0 \pm 25$   | $9.38 \pm 2.15$   | $13.22 \pm 1.06$  | 0.910 | 0.15            | $\sim 150.1$      |
| C4  | 0.3 | $3.5 \pm 6.5$    | $14.37 \pm 28.31$ | $19.34 \pm 26.60$ | 0.796 | 0.13            | $\sim 317.3$      |
| C5  | 0.4 | $-21.0 \pm 12$   | $30.15 \pm 44.86$ | $38.98 \pm 38.02$ | 0.742 | 0.11            | $\sim 729.7$      |
| C6  | 0.4 | $-7.5 \pm 0.5$   | $10.14 \pm 14.44$ | $17.30 \pm 19.88$ | 0.724 | 0.23            | $\sim 70.8$       |
| C7  | 0.4 | $-14.5 \pm 8.5$  | $16.97 \pm 3.96$  | $50.63 \pm 16.17$ | 0.866 | 0.47            | $\sim 593.3$      |
| C8  | 0.3 | $13.0 \pm 12$    | $16.33 \pm 19.44$ | $17.05 \pm 6.46$  | 0.802 | 0.02            | $\sim 788.5$      |
| C9  | 0.4 | $-66.5 \pm 12.5$ | $10.29 \pm 6.94$  | $18.47 \pm 9.01$  | 0.807 | 0.25            | $\sim 453.2$      |
| C10 | 0.3 | $-66.5 \pm 11.5$ | $10.40 \pm 4.71$  | $16.78 \pm 4.30$  | 0.885 | 0.21            | $\sim 229.6$      |

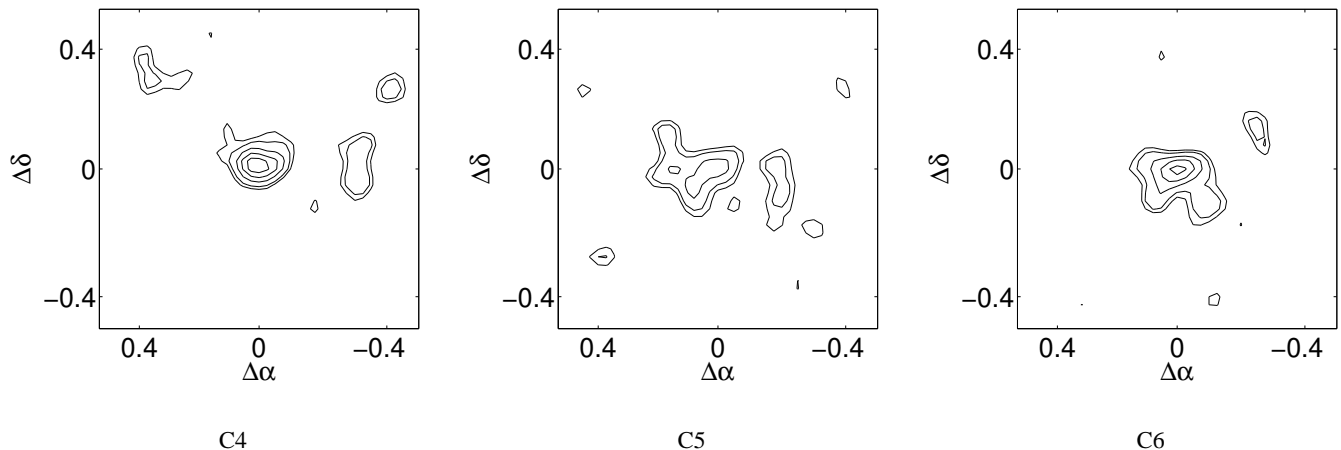
Notes: e=ellipticity, pa=position angle,  $R^2$ =related coefficient



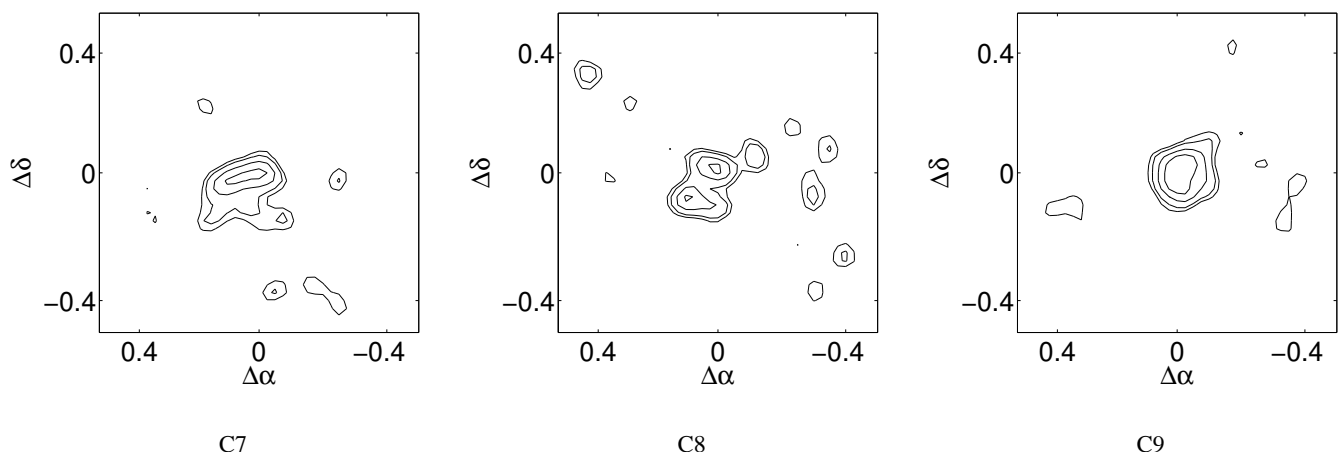
**Fig. 2.** The last five overdensities labeled from C6 to C10.



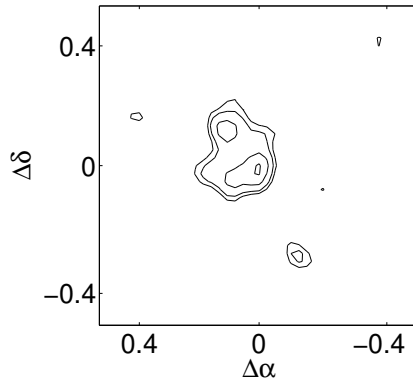
**Fig. 3.** Isodensity contours of overdensities C1, C2 and C3. The contour levels are 1.5, 2, 3, 4, 5 and  $7\sigma$  above the background. The samples generated to the contours are selected by corresponding Hess diagram.



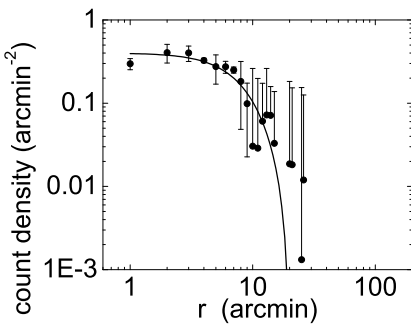
**Fig. 4.** Isodensity contours of overdensities C4, C5 and C6.



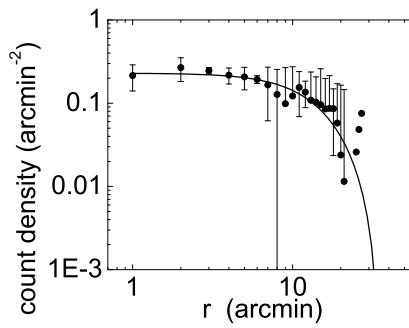
**Fig. 5.** Isodensity contours of overdensities C7, C8 and C9.



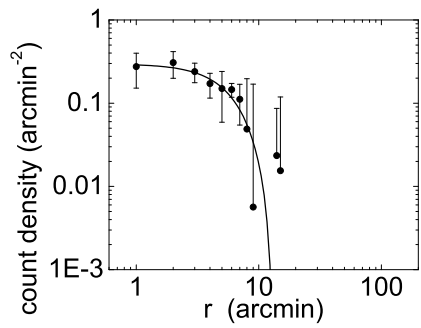
C10

**Fig. 6.** Isodensity contours of overdensities C10.

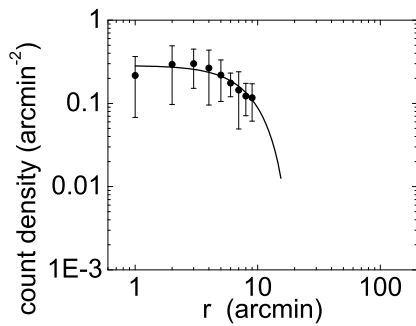
C1



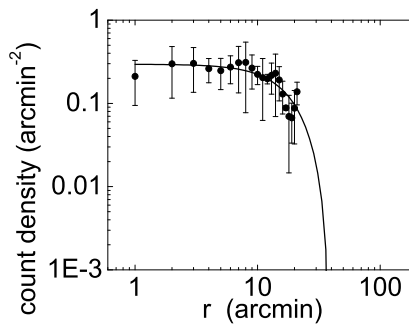
C2



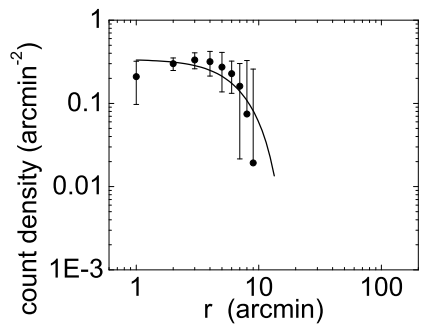
C3

**Fig. 7.** Density radial profiles along with major axis for C1, C2 and C3.

C4



C5



C6

**Fig. 8.** Density radial profiles along with major axis for C4, C5 and C6.

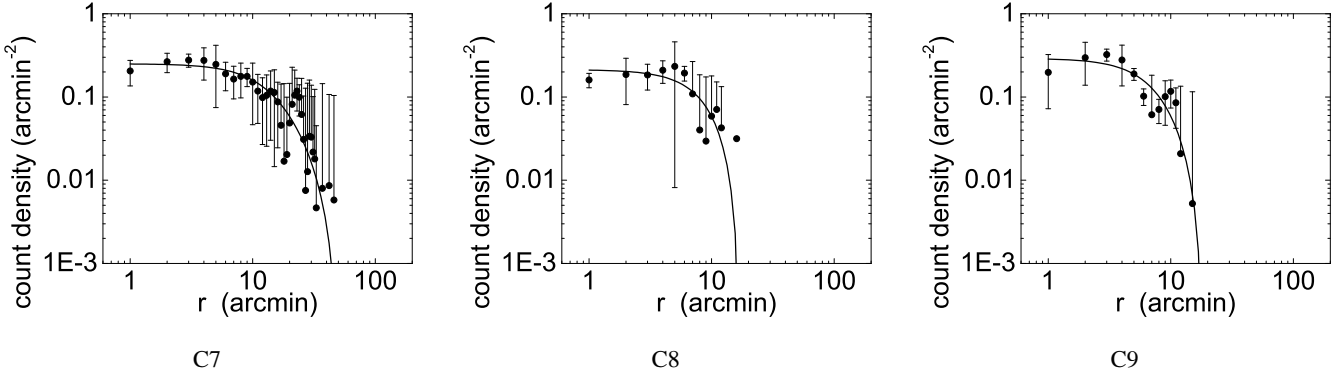


**Fig. 9.** Density radial profiles along with major axis for C7, C8 and C9.

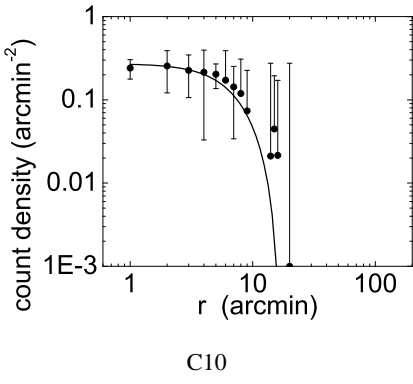


**Fig. 10.** Density radial profiles along with major axis for C10.

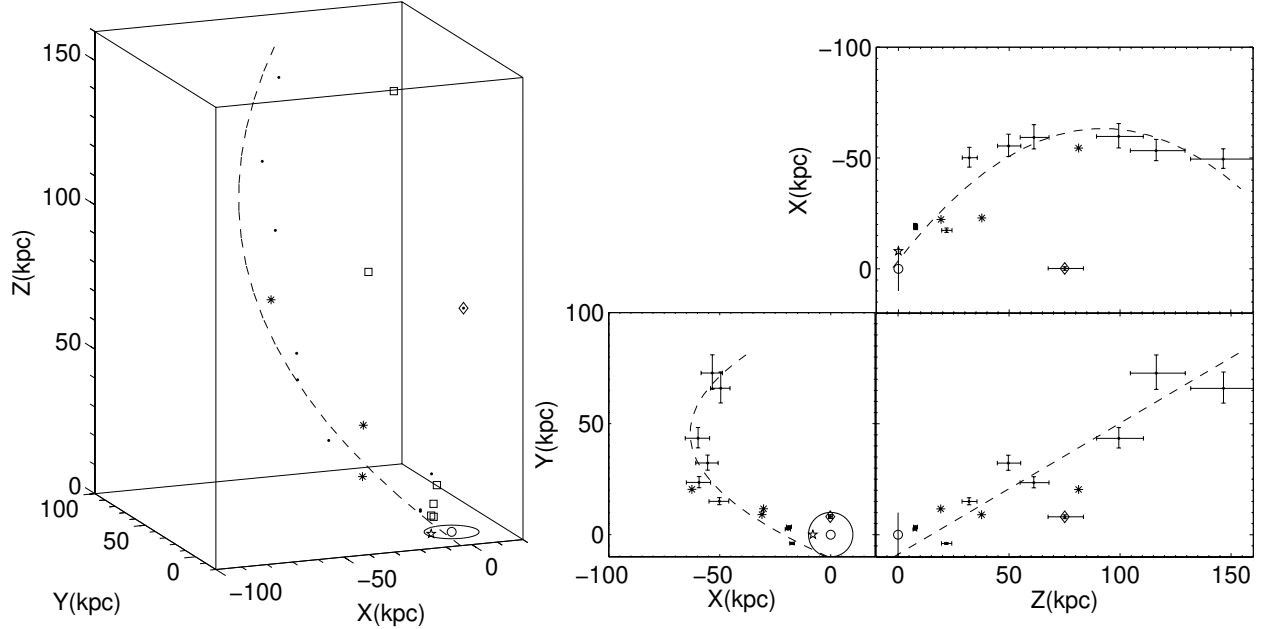


**Fig. 11.** The left diagram is a 3D space plotting for overdensities and known satellites. The pentagon stands for the Sun and a small circle stands for the galactic center. The bigger circle represents the Milky Way's disk with a radius of 10kpc. The round dots along the dash line from the disk(bottom) to the halo(top) are C1, C2, C6, C3, C4, C5, C7, C9 and C8. The diamond spot is C10. Star symbols from bottom to top represent for the position of UMa II, Willman 1 and UMa I. Rectangle symbols represent for CVn I & II, Pal4, NGC5272, NGC6205, NGC5466, and NGC6341. A dash curve shows the fitted 2-order polynomial curve of C1-C9, UMa I & II and Willman 1. The right three diagrams are XY XZ and YZ plane projections. Distance measure errors are decomposed to XYZ axis and showed as error bars cross the round dots. In YZ and XZ plane, the Galaxy is edging on. Thus disk are represented by a short line with length of 20kpc.

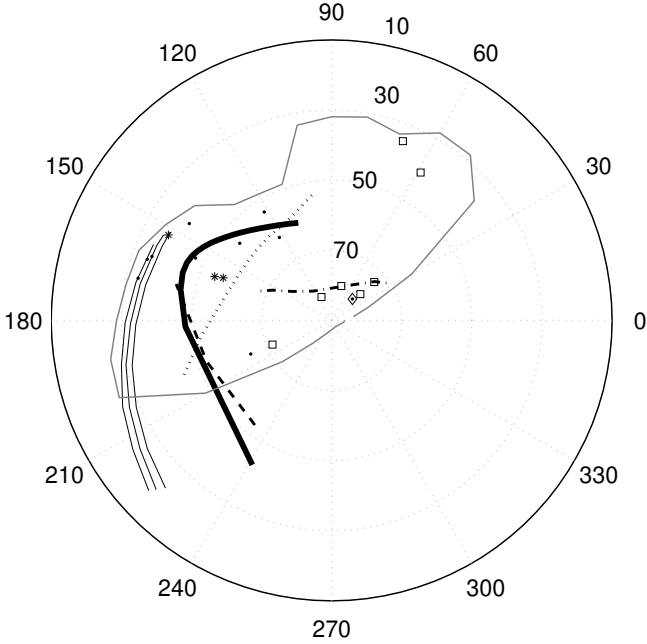


**Fig. 12.** The new arc structure and overdensities' positions in galactic coordinates. The center of the diagram is Galactic North Pole. The solid line polygon encloses the area we detected in the SDSS DR5 data. Dots along the clockwise direction from  $l = 210^\circ$  are C6, C1, C2, C3, C4, C7, C8, and C9. Diamond point is C10. Star points from outside to the north pole are UMa II, Willman 1 and UMa I. Squares are Pal4, NGC5272, NGC5466, NGC6205, NGC6341, CVn I and CVn II. Thick solid line is the fitted curve using C1-C9, UMa I & II and Willman I. The triple lines are Monoceros Ring. The dot line is GD-1. The dash line is Orphan stream. The dash-dot line is NGC5466's tidal stream.

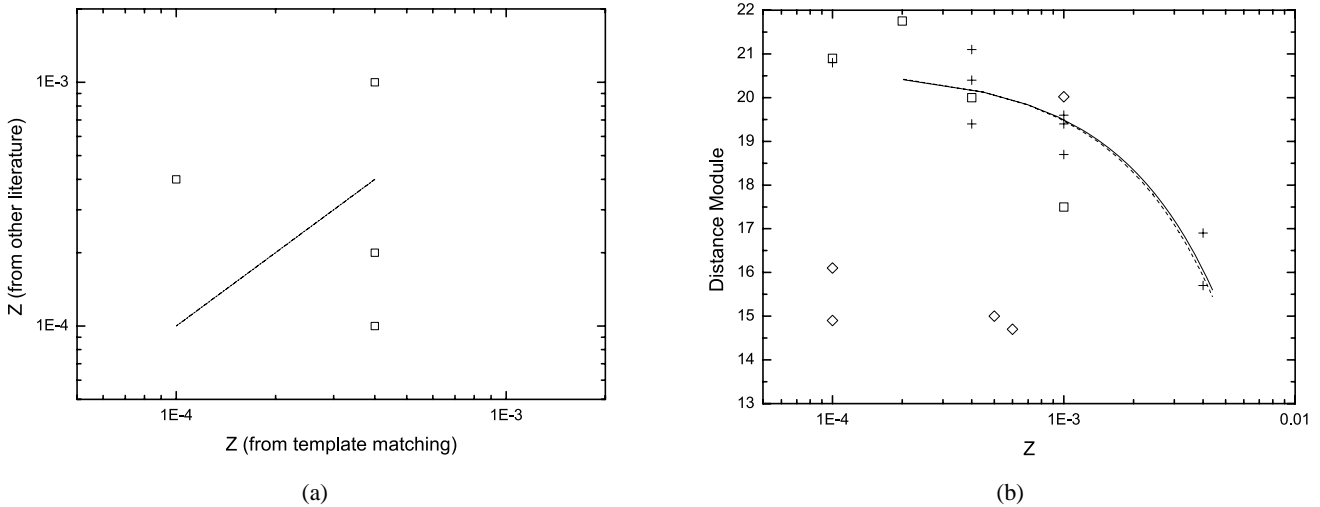


**Fig. 13.** (a) Metalicity estimation test using four known objects, UMa I, UMa II, CVn I and CVn II. This shows that the template matching method mentioned in this paper can be used to estimate the order of the metalicity. The line is the bisector. (b) Relationship between metalicity and distance module of the overdensities and known galaxy satellites. The cross symbols shows ten overdensities. Their metalicity are provided by the template matching method. The rectangle symbols are 4 dwarf spheroidal galaxies, UMa I, UMa II, CVn I, and CVn II. The diamond symbols are 5 globular clusters, NGC5272, NGC5466, NGC6205, NGC6341 and Pal4. Their metalicities come from related literatures (Zucker et al. 2006b; Willman et al. 2005a; Belokurov et al. 2006d; Zucker et al. 2006a; Stetson et al. 1999 and Harris 1996). The solid line is the fitted line of ten overdensities. The dashed line is the fitted line of both 10 overdensities and 4 known dSphs. They are almost identical which implies that the relationship of the metalicity and distance are highly consistent with our ten overdensities and known dSphs. However, globular clusters seem not comply with the same rule.